Journal of Magnetic Resonance **138,** 107–114 (1999)
Article ID jmre.1999.1714, available online at http://www.idealibrary.com on IDEAL®

Evaluation of Slaved Pulses to Study Protein Hydration

Olivier Bornet,* Françoise Guerlesquin,* and Martial Piotto†

**IBSM-CNRS, 31, chemin Joseph Aiguier, F-13402 Marseille Cedex 20, France; and †UMR 7510 CNRS-Bruker, 34, rue de l'industrie, F-67166 Wissembourg, France*

Received September 15, 1998; revised December 21, 1998

The new concept of slaved pulses is evaluated in the context of the study of protein hydration. The inversion properties of these pulses are shown to be superior in quality to the previously published schemes. High-quality water selective homonuclear 2D ^{1}H NOESY–NOESY and NOESY–TOCSY experiments were recorded on horse heart ferrocytochrome *c*. © 1999 Academic Press

Key Words: **selective water inversion; radiation damping; feedback field; slaved pulses; ferrocytochrome *c*; protein hydration.**

INTRODUCTION

Since the pioneering work of Otting and Wüthrich (*1–5*), which proved the feasibility of studying protein hydration by NMR, extensive work has been directed in this area. Detecting NOEs or ROEs between water molecules and protein protons allows the precise location of the bound water molecules to be determined and sheds additional light on the structure and function of the protein.

Whereas the initial studies were conducted using 3D ^{1}H homonuclear experiments, it quickly became apparent that these methods were too time-consuming and that they could advantageously be replaced by water selective 2D ^{1}H homonuclear experiments (*6*, *7*).

These experiments rely on the selective excitation of water magnetization, which is then subjected to a first mixing period, during which part of the water magnetization is transferred through chemical exchange or dipolar cross relaxation to protein protons. In order to help in the assignment process, a second mixing period is usually included to provide a second dimension. In practice, the most commonly used water selective homonuclear 2D experiments are NOESY–NOESY, NOESY–TOCSY, ROESY–NOESY, and ROESY–TOCSY.

The main difficulty in these experiments consists of properly and selectively exciting the intense water resonance. The phenomenon of radiation damping (*8*) will tend to counteract the effect of the selective pulse and to bring the water magnetization back along the $+Z$ axis, therefore preventing a good inversion of the water signal. A lesser degree of water excitation means that less water is available for NOE, ROE, or exchange transfers and that the resulting 2D spectra will be of poorer quality. This phenomenon becomes more pronounced with increasing magnetic fields.

Several solutions have been proposed in the literature to overcome this problem, including the use of Q-switched probes (*9, 10*) and the use of bipolar gradients between the successive points of a shaped pulse (*11*). Currently, the most popular approach, proposed by Dalvit *et al.* (*12, 13*), is based on a selective spin echo. This approach uses a 180° water selective pulse surrounded by two identical gradients to select the transverse magnetization of the water signal. In order to achieve sufficient selectivity, a 50-ms Gaussian pulse is usually employed. This sequence is particularly easy to implement and produces high-quality spectra; however, as will be seen below, it is very sensitive to diffusion and relaxation effects.

RESULTS AND DISCUSSION

In this article, we evaluate a radically different approach for selectively inverting the water signal which is based on the control of radiation damping by an electronic circuit (*14–17*). Briefly, the principle of this technique is to use an electronic device that can detect the water signal and subject it to the following manipulations. The signal is first demodulated to audio frequency, then filtered at the water frequency, and finally remodulated before being fed back into the probe with the appropriate phase and amplitude. A detailed description of the system can be found in Refs. (*14*) and (*16*). The feedback field is water-magnetization-dependent and is a faithful image of the transverse water magnetization present in the sample. In this manner, depending on the phase of the feedback signal, it is possible to cancel or to accelerate radiation damping. A particularly useful application of this system, which was originally proposed by the group of Jean-Yves Lallemand (*18*), is to invert the water signal very efficiently. In order to achieve that purpose, the feedback field must satisfy two conditions: its phase must be shifted by 180° with respect to the radiation damping field and its intensity must be superior to that of the radiation damping field. The overall effect is therefore not to bring the water magnetization along the $+Z$ axis but along the $-Z$ axis (*18*). Practically, starting from equilibrium magnetization, a short nonselective RF pulse that slightly tilts the magnetization away from equilibrium generates enough transverse water magnetization to initiate the inversion process. The nonselective pulse is applied using the standard proton channel

1090-7807/99 $30.00

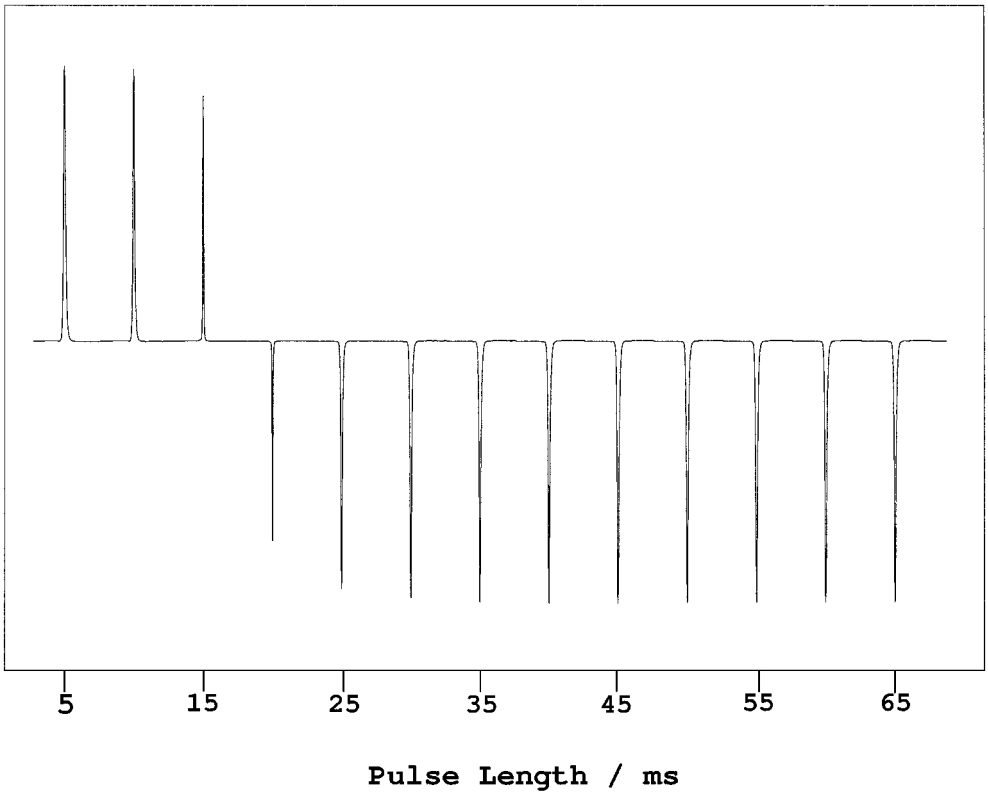

FIG. 1. Pulse calibration of an inversion slaved pulse ($+M_z \rightarrow -M_z$). The pulse is incremented from 5-ms by 5-ms steps (see legend to Fig. 3 for the actual pulse scheme and experimental details).

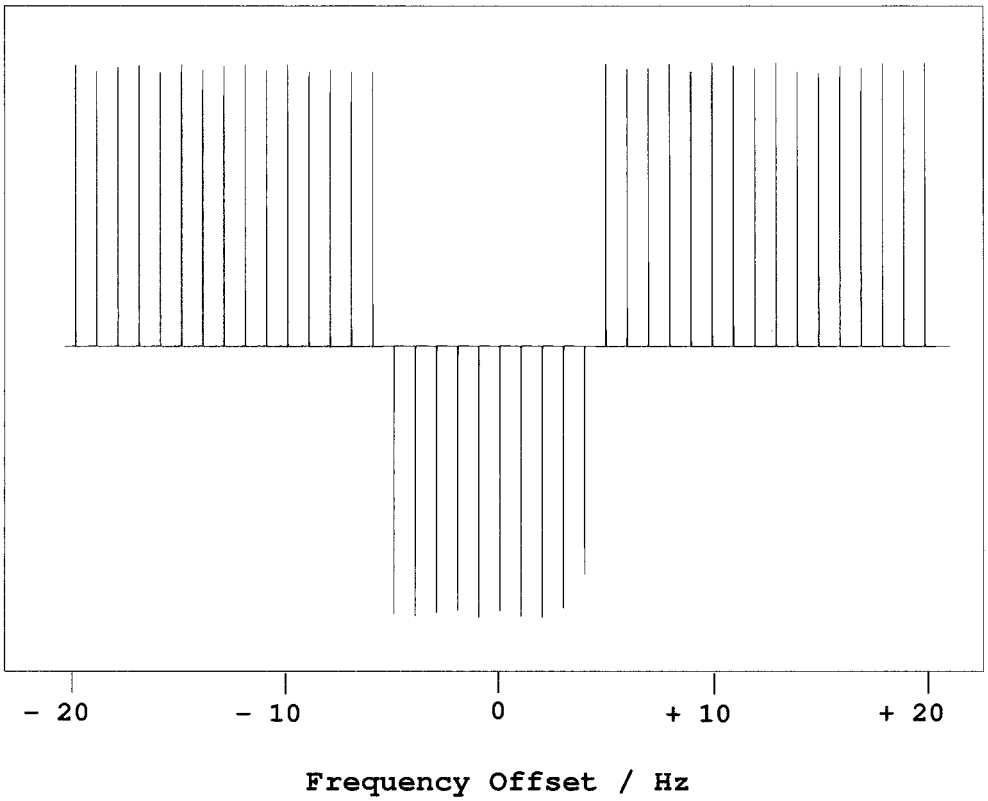

FIG. 2. Inversion profile ($+M_z \rightarrow -M_z$) of a 40-ms slaved pulse. The profile was obtained by varying the remodulation frequency in 1-Hz increments (see legend to Fig. 3 for the actual pulse scheme and for experimental details).

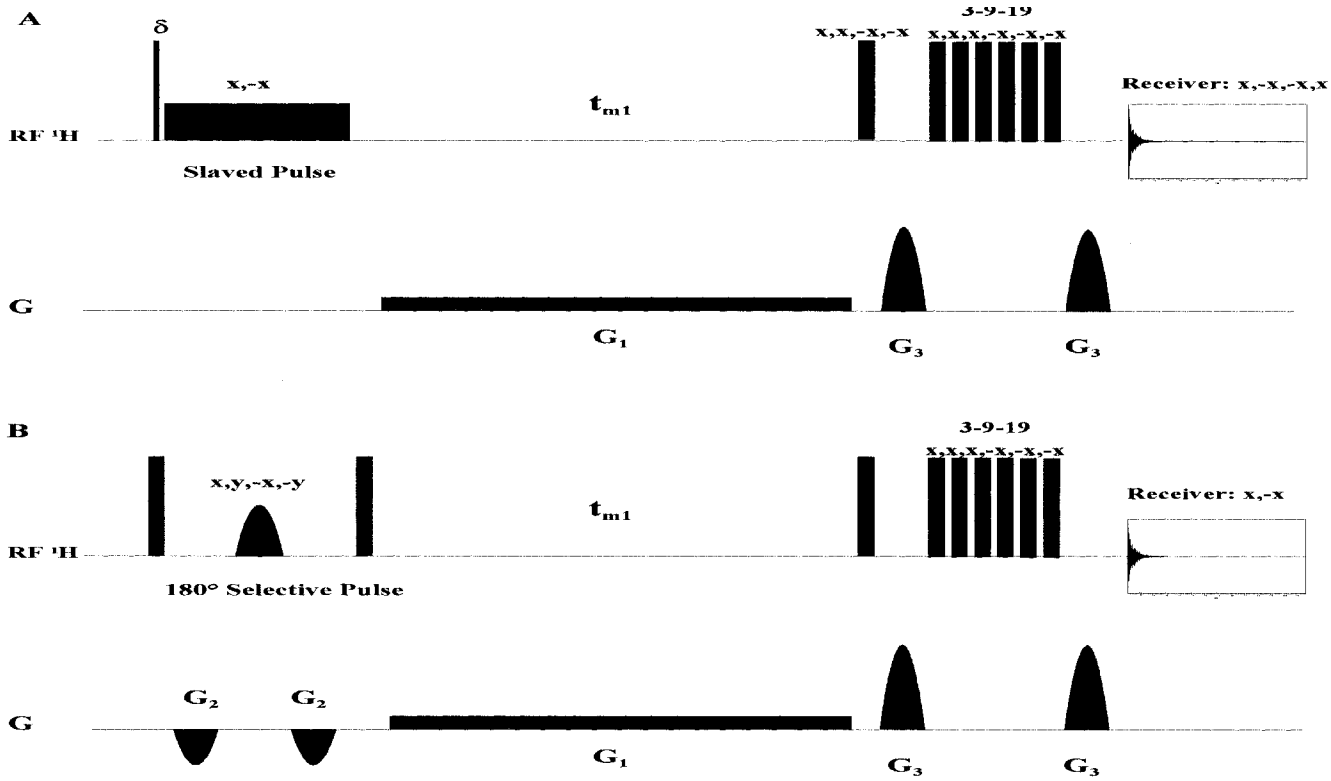

FIG. 3. (A) Water selective 1D NOESY experiment using a slaved pulse to invert the water signal. The δ pulse is a short nonselective pulse of about 3° and the slaved pulse is applied over 40 ms using a separate channel of the spectrometer that contains the radiation damping control board. According to the phase of the slaved pulse, the water magnetization is either brought to the $-Z$ axis (phase $+x$) or to the $+Z$ axis (phase $-x$). The phase of the pulses is $+x$ unless indicated otherwise. The gradient $G1$ prevents radiation damping during t_{m1} (*19*). Water suppression is achieved through a Watergate block (*20, 21*). (B) Water selective 1D NOESY experiment using a selective spin echo (*12, 13*). A 180° Gaussian pulse of length 50 ms is used to select the water magnetization.

of the instrument whereas the feedback pulse is generated using a separate channel that contains the radiation damping board. Since, as explained previously, the two pulses must bear a definite phase relationship, a perfect phase coherence must exist between the two channels of the spectrometer used for the experiment. This requirement is, however, not a handicap since it is a standard feature of modern spectrometers.

This technique allows all of the water signal to be inverted very efficiently leading to spectra with enhanced sensitivity. The nature of the feedback pulse compared to that of classical RF pulses commonly used in NMR is very peculiar. As described by Abergel (*18*), the shape, the phase, and the amplitude of the feedback pulse are solely water-magnetization-dependent. The pulse can be thought of as slaved to the water magnetization. It has the very intriguing and interesting property of dropping to zero intensity as soon as the water is along the $+Z$ or $-Z$ axis. In that case, the projection of the water magnetization onto the (x, y) plane is close to zero and the slaved pulse almost vanishes.

The pulse calibration of Fig. 1 reveals some interesting features as to the way these pulses operate. In that example, the water is entirely inverted after 40 ms and the transition region is quite narrow. This is an interesting property since transient NOE effects that occur during the pulse will be reduced. As mentioned previously, once the slaved pulse has inverted the water magnetization, its intensity drops to a very small value that is sufficient to maintain the water magnetization along the $-Z$ axis. An immediate advantage is that these pulses are not very sensitive to pulse misadjustment. Once past a given threshold for the pulse length, the water always ends up along the $-Z$ axis. As mentioned previously, in order to achieve water inversion, the slaved pulse must have a well-defined phase with respect to the initial short nonselective pulse. However, the phase setting is not critical and water inversion occurs with the same efficiency over a 40° range (data not shown). The pulse calibrations are obviously probe- and sample-dependent since the intensity of the radiation damping field depends on the Q factor of the probe and on the quantity of H_2O present in the sample. The quality of the inversion is quite satisfactory since the integral of the inverted water signal using a 40-ms slaved pulse is equal to 85% of the signal recorded with a nonselective 90° pulse.

The slaved pulse has the very valuable property of being extremely selective. An excitation profile recorded by keeping the demodulation frequency constant and by stepping the remodulation frequency in 1-Hz steps is shown in Fig. 2. These data show that a 40-ms slaved pulse exhibits a selectivity of 10 Hz with very sharp transition regions. The 50-ms Gaussian

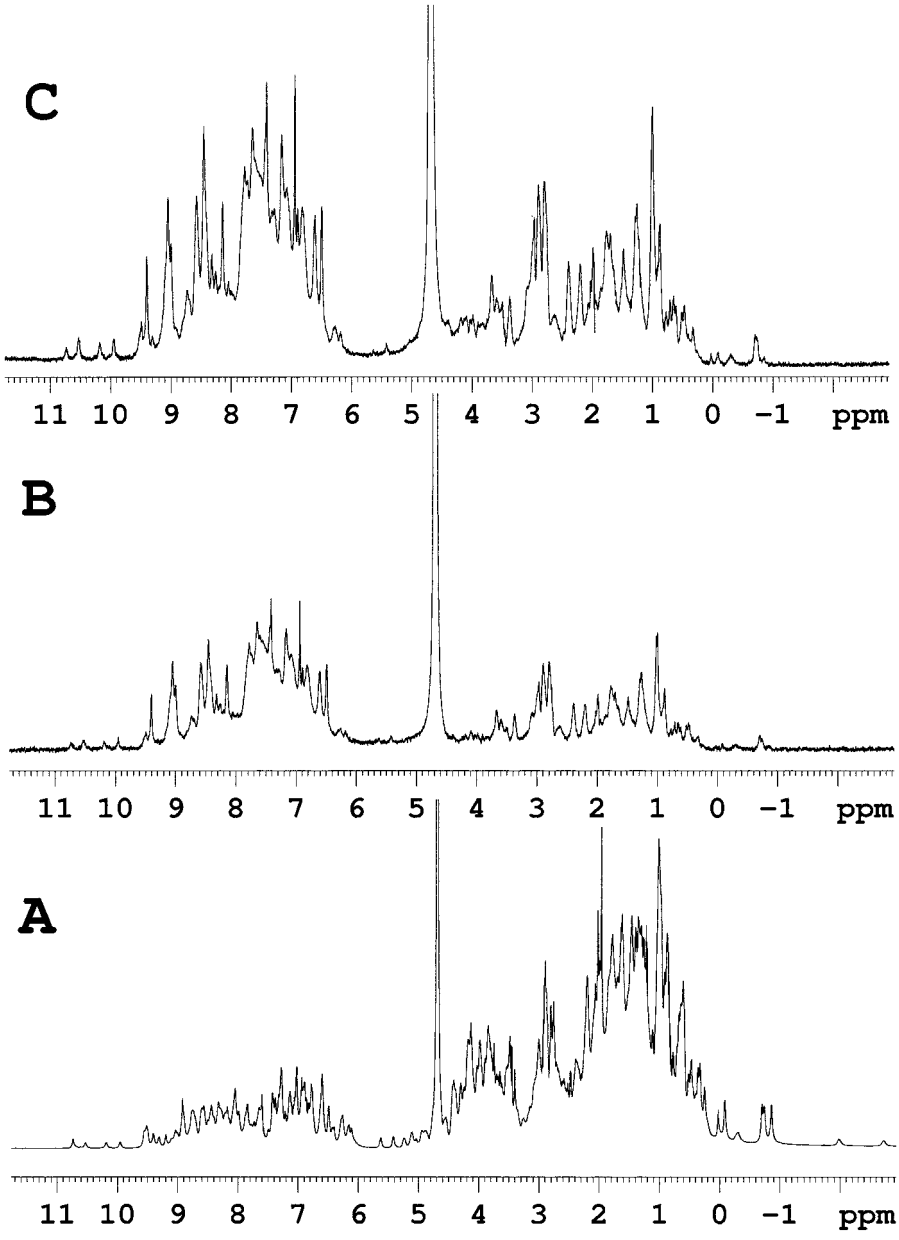

FIG. 4. Comparison of the results obtained with the two sequences of Fig. 3 on a 10 mM sample of horse heart ferrocytochrome *c* in 90% H_2O and 10% D_2O, containing 50 mM phosphate buffer (pH 5.9) at 300 K. A 500-MHz DRX Bruker spectrometer equipped with a HCN probe and self-shielded triple axis gradients was used. (A) Reference 1D spectrum recorded with 8 scans and presaturation. (B) Spectrum recorded with the sequence shown in Fig. 3B with 64 scans and a 100-ms mixing time. A 50-ms Gaussian pulse was used to select the water magnetization. The strength of the 1-ms gradients $G1y$, $G2x$, and $G3x$ was 0.25, −5, and 20 G cm^{-1}, respectively. (C) Spectrum recorded with the sequence shown in Fig. 3A using 64 scans, a 40-ms slaved pulse, and a 100-ms mixing time. The strength of the 1-ms gradients $G1y$ and $G3x$ was about 0.25 and 20 G cm^{-1}, respectively.

pulse typically used in Dalvit's experiment has a selectivity of about 40 Hz.

In order to check the relative performances of these two water inversion schemes, the pulse sequences of Fig. 3 were used to record water selective 1D NOESY experiments. In Fig. 3A, the pulse sequence using a slaved pulse is described. δ is the small nonselective pulse that precedes the actual slaved pulse. According to the phase of the slaved pulse, the water magnetization is either inverted (phase $+x$) or brought back along the $+Z$ axis (phase $-x$). By taking the difference between the two spectra, only the protons in interaction with water (chemical exchange or dipolar effects) are selected. To increase the efficiency of the magnetization transfer between the water molecules and the protein, a constant gradient of strength $G1$ is applied during the whole mixing time (*19*). This gradient suppresses radiation damping and allows the water magnetization to be kept along the $-Z$ axis during the whole mixing time. Water suppression is achieved by a Watergate

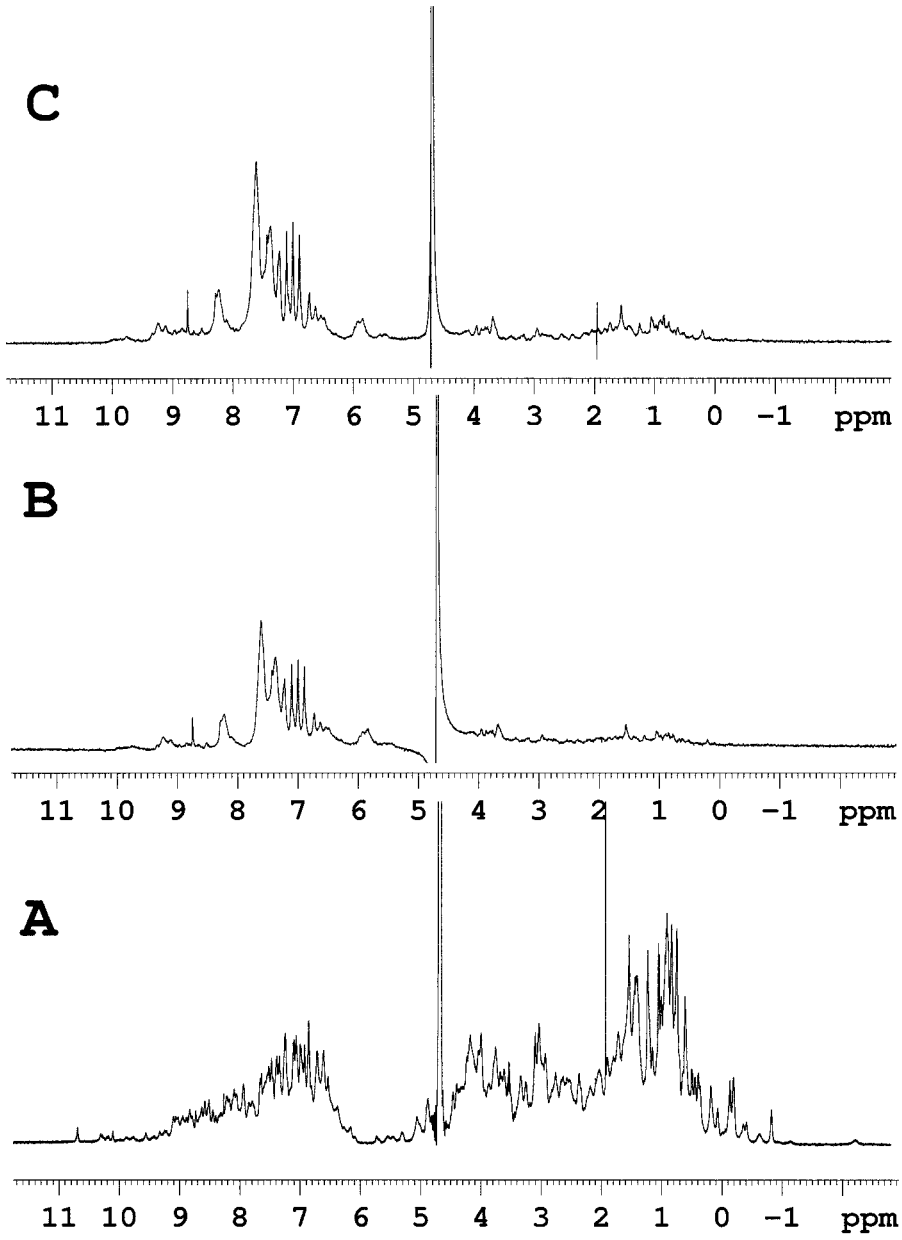

FIG. 5. Comparison of the results obtained with the two sequences of Fig. 3 on a 2 mM sample of lysozyme in 90% H_2O and 10% D_2O under the same conditions as Fig. 4. (A) Reference 1D spectrum recorded in 8 scans with presaturation. (B) Spectrum recorded using the sequence of Fig. 3B with 128 scans and a 100-ms mixing time. (C) Spectrum recorded using the sequence shown in Fig. 3A with 128 scans, a 40-ms slaved pulse, and a 100-ms mixing time.

block (*20*, *21*) prior to detection. Figure 3B describes the water selective 1D NOESY experiment using a selective gradient echo. The phase cycling of the 180° selective pulse brings the water alternatively along the $+Z$ axis or along the $-Z$ axis. The difference between the two spectra shows again only the protons in interaction with water. Apart from the inversion scheme, the two sequences are identical. The sequence of Fig. 3A is potentially more sensitive to subtraction artifacts resulting from instrument instability since the signals of the nonexchangeable protons have to be suppressed completely by the phase cycling. Figure 3B, on the other hand, defocuses these signals before the mixing time, therefore minimizing the intensity of the signals that have to be subtracted. These signals can, however, relax during the mixing time (t_{m1}) and reach an important intensity when long mixing times are used. Dipolar field effects (*22*) can also affect the quality of the subtraction process; however, control experiments (*23*) run with a short mixing time (1 ms) show only signals originating from fast exchangeable protons and no protein signals in the aliphatic region, proving the quality of the subtraction process.

The results obtained on a 10 mM ferrocytochrome *c* sample in 90% H_2O (Fig. 4) show clearly that the two pulse sequences

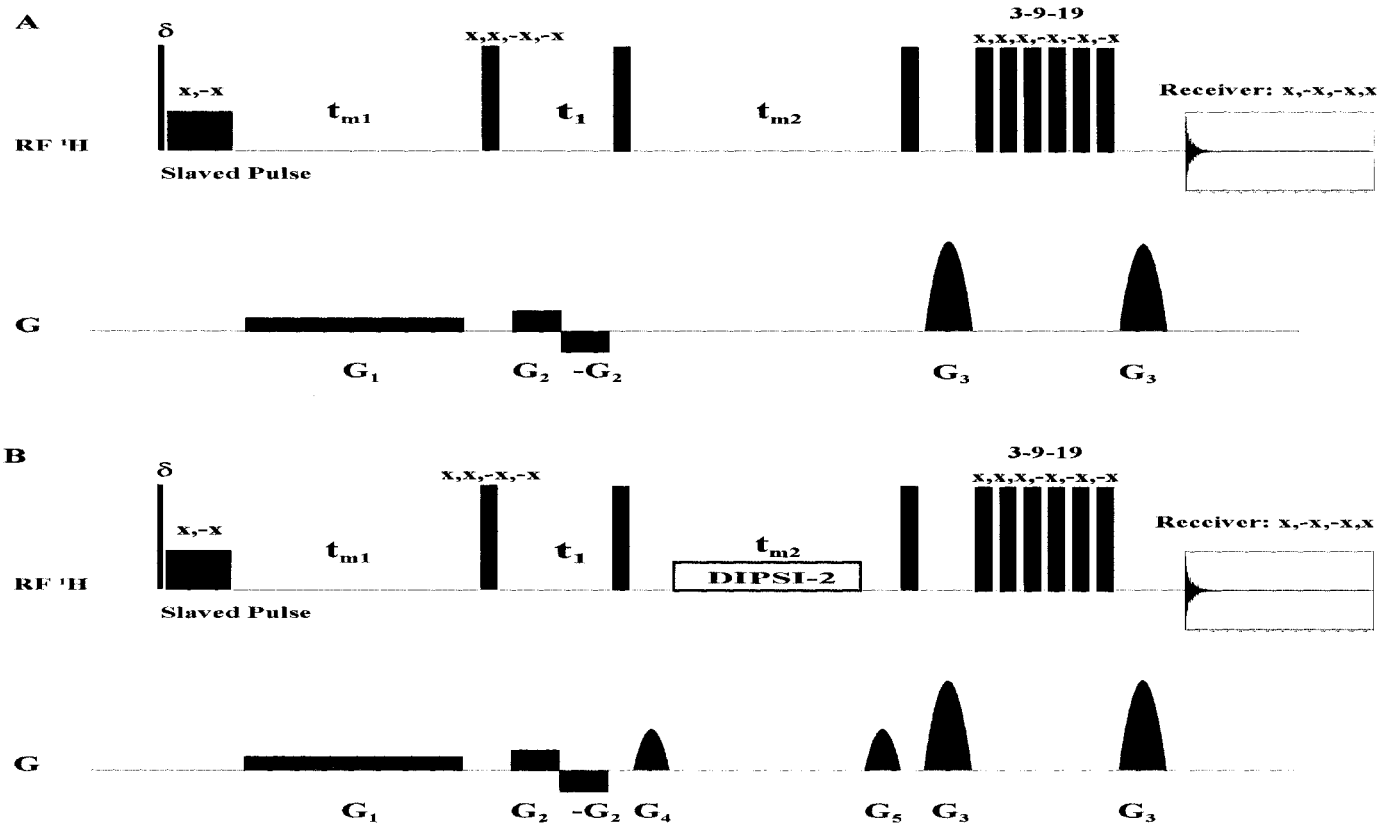

FIG. 6. Pulse sequences used for the water selective 2D NOESY–NOESY (A) and NOESY–TOCSY (B) experiments with slaved pulses. The δ pulse is a short nonselective pulse of about 3° and the slaved pulse is applied over 40 ms. The three pulses that surround t_1 and t_{m2} are 90° pulses. The phase of the pulses is $+x$ unless indicated otherwise. The gradients $G1$, $G2$, and $-G2$ prevent radiation damping during t_{m1} and t_1, respectively (*19*). $G4$ and $G5$ are used to select Z magnetization. Water suppression is achieved through a Watergate block (*20, 21*). Quadrature detection in $f1$ is achieved using the States–TPPI method (*28*). The TOCSY mixing is achieved with a DIPSI-2 sequence (*29*).

produce artifact-free spectra with the same information content. However, it is immediately clear that the spectrum recorded with a slaved pulse exhibits a signal-to-noise improvement that approaches a factor of 2. This important difference in signal-to-noise originates from diffusion or/and relaxation effects taking place during the 50-ms Gaussian pulse. In order to differentiate between the two effects, spectra were recorded with different gradient strengths to select the water signal (gradient $G2$ in Fig. 3B). The results show that there is not a significant improvement in signal-to-noise when weaker gradients are used, therefore excluding diffusion effects. The origin of the loss of signal-to-noise is therefore due to relaxation processes. It is indeed known that the T_2 relaxation time of water protons in the presence of a compound with exchangeable protons can be shorter than 200 ms due to exchange broadening (*5*). The presence of a small amount of paramagnetic compounds will create a similar decrease of the value of the T_2 relaxation time of water. In the case of the ferrocytochrome *c* sample, the length of the 180° Gaussian selective pulse had to be reduced to a value inferior to 12 ms in order to achieve the same signal-to-noise as the one obtained with the experiment using a slaved pulse. To check how the two excitation schemes compared on different protein samples, the same experiments were run on a 2 mM lysozyme sample. The results of Fig. 5 show this time a more modest increase in signal-to-noise of the order of 15–20%. These measurements therefore indicate a very different relaxation behavior of the water protons in lysozyme and in ferrocytochrome *c*. A subtraction artifact is visible in Fig. 5C at around 2 ppm and appears as a dispersive lineshape. This peak corresponds to a narrow acetate peak (half width of 2 Hz) and is therefore the most likely to be affected by subtraction artifacts. The broader protein resonances (10–30 Hz) all appear as absorptive lineshapes.

The inversion scheme using a slaved pulse was incorporated into a water selective 2D NOESY–NOESY and a water selective 2D NOESY–TOCSY experiment as shown in Fig. 6. The experiment starts with the same module as the one used by the 1D NOESY experiment and continues with a t_1 labeling period during which radiation damping is canceled using bipolar gradients (*19*). A second mixing time of length t_{m2} follows that can be either a second NOESY mixing (Fig. 6A) or a TOCSY mixing (Fig. 6B). Since the NOE transfer will take place within the proton network of the protein, there is no need to suppress

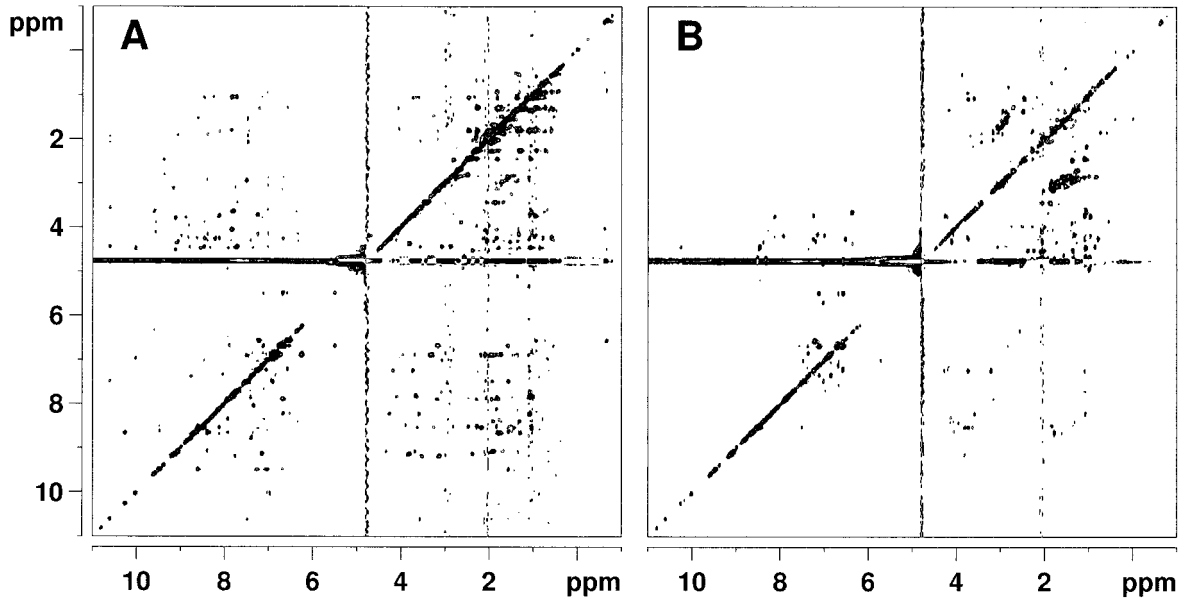

FIG. 7. Water selective 2D NOESY–NOESY (A) and NOESY–TOCSY (B) spectra recorded with the pulse sequences of Figs. 6A and 6B, respectively, using a 40-ms slaved pulse. Spectra were acquired at 300 K on a 10 mM sample of horse heart ferrocytochrome *c* in 90% H_2O and 10% D_2O, containing 50 mM phosphate buffer (pH 5.9). Sixty-four scans were recorded for each of the 256 t_1 increments. The gradients $G1y$, $G2x$, $G3x$, $G4z$, and $G5z$ had a strength of 0.25, 0.5, 20, 5, and -8 G cm^{-1}, respectively. The NOESY mixing time t_{m1} was set to 100 ms and the NOESY and the DIPSI-2 mixing times t_{m2} were set to 100 and 50 ms, respectively. The spectral width in both dimensions was 8500 Hz. The data were multiplied with a cosine bell square function in both dimensions, prior to Fourier transformation. Linear prediction up to 512 data points was applied in dimension $f1$. The interscan delay was 2 s, the total recording time was around 10 h.

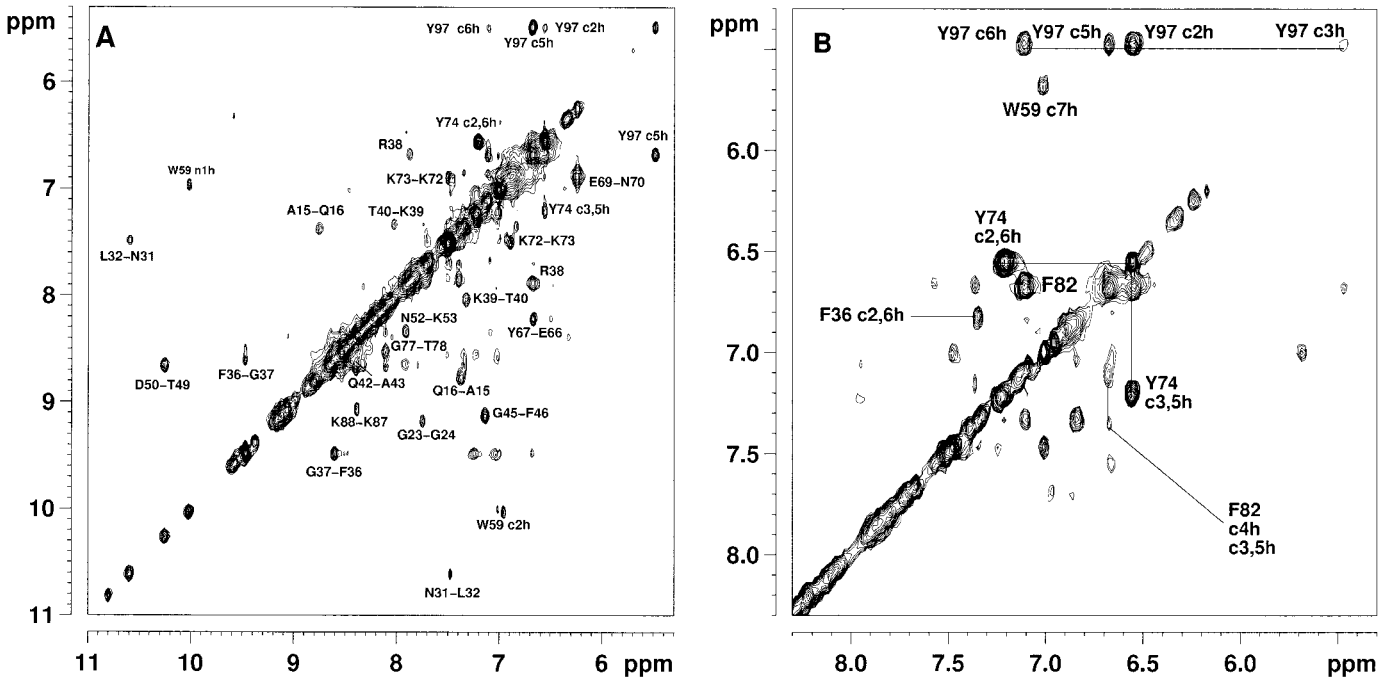

FIG. 8. Expansion of the water selective 2D NOESY–NOESY (A) and NOESY–TOCSY (B) spectra recorded on the horse heart ferrocytochrome *c* sample. Resonance assignments of ferrocytochrome *c* are based on previously published data (*22*). Residues in interaction with water molecules are indicated. The diagonal peaks arise from the transfer of magnetization from the water to protein resonances during the first NOESY mixing time (t_{m1}) whereas the cross peaks originate from a second magnetization transfer during the second mixing time (t_{m2}). Transfers occur among scalar-coupled protons during the TOCSY mixing period or among dipolar-coupled protons during the NOESY mixing period.

radiation damping with a gradient pulse. Water suppression is again achieved by a Watergate block (*20, 21*) prior to detection.

These 2D pulse sequences were applied to the 10 mM horse heart ferrocytochrome *c* sample at 300 K. Figure 7A shows the result of the water selective 2D NOESY–NOESY and Fig. 7B the result of the water selective 2D NOESY–TOCSY. The quality of these experiments is remarkable with very few artifacts and a high signal-to-noise ratio. The only visible artifact appears as t_1 noise around 2 ppm and is the result of an incomplete cancellation of the acetate peak present in the sample. Similar spectra recorded using Dalvit's method show the same cross peaks but with an intensity that is inferior by a factor of 2.

The previous data were analyzed using the proton assignments previously published by Wand and Di Stephano (*24*). An expansion of the water selective 2D NOESY–NOESY spectrum (Fig. 8A) allows the easy identification of amide protons (A15, Q16, G23, N31, L32, F36, G37, K39, T40, Q42, G45, N52, Y67, E69, K72, K73, G77, K88), NH_2 groups (R38), and aromatic ring protons (W59, Y74, and Y97) of ferrocytochrome *c* residues found in contact or in chemical exchange with water molecules. These data are consistent with the previously published data on the hydrating water molecules in solution structure of horse ferrocytochrome *c* (*25*) and crystallographic data on yeast ferrocytochrome *c* (*26, 27*). In these structures, K39, T40, Q42 NHs, and R38 NH_2 interact with Wat121, Q16 NH is close to Wat126, N52 and Y67 NHs are in the vicinity of Wat166, and K72 and F36 NHs interact with Wat172 and Wat196, respectively. Moreover, R38 side chain protons, W59 ring protons, and N31 and L32 NHs are in interaction with Wat168 in yeast cytochrome *c*.

In the NOESY–TOCSY experiment, the ring protons of aromatic residues in interaction (NOE or chemical exchange) with water molecules are particularly well observed (Fig. 8B). As noticed previously, these data are consistent with the proximity of W59 to Wat168, F36 to Wat 124, and F82 to Wat107.

CONCLUSIONS

In this article, we have shown the ability of slaved pulses to invert very efficiently and selectively the water magnetization thereby generating 2D NOESY–NOESY and NOESY–TOCSY spectra with high signal-to-noise. Slaved pulses are, however, not limited to inversion processes and they can also be used as 90° excitation pulses. The study of their implementation in 2D ROESY–NOESY and ROESY–TOCSY experiments is currently under investigation.

ACKNOWLEDGMENT

Very valuable discussions with Dr. C. Dalvit are gratefully acknowledged.

REFERENCES

1. G. Otting and K. Wüthrich, *J. Am. Chem. Soc.* **111,** 1871 (1989).
2. G. Otting, E. Liepinsh, and K. Wüthrich, *Science* **254,** 974 (1991).
3. G. Otting, E. Liepinsh, B. T. Farmer II, and K. Wüthrich, *J. Biomol. NMR* **1,** 209 (1991).
4. G. Otting, E. Liepinsh, and K. Wüthrich, *J. Am. Chem. Soc.* **114,** 7093 (1992).
5. G. Otting, *Prog. NMR Spectrosc.* **31,** 259 (1997).
6. R. W. Kriwacki, R. B. Hill, and J. P. Flanagan, J. *J. Am. Chem. Soc.* **115,** 8907 (1993).
7. S. Mori, M. O. Johnson, J. M. Berg, and P. C. M. van Zijl, *J. Am. Chem. Soc.* **116,** 11982 (1994).
8. A. Abragam, "The Principles of Nuclear Magnetism," Clarendon Press, Oxford (1961).
9. G. Otting and E. Liepinsh, *J. Magn. Reson. B* **107,** 192 (1995).
10. C. Anklin, M. Rindlisbacher, G. Otting, and F. H. Laukin, *J. Magn. Reson. B* **109,** 218 (1995).
11. A. Böckmann and E. Guittet, *J. Biomol. NMR* **8,** 87 (1996).
12. C. Dalvit and U. Hommel, *J. Magn. Reson. B* **109,** 334 (1995).
13. C. Dalvit, *J. Magn. Reson. B* **112,** 282 (1996).
14. A. Louis-Joseph, D. Abergel, and J-Y. Lallemand, *J. Biomol. NMR* **5,** 212 (1995).
15. D. Abergel, C. Carlotti, A. Louis-Joseph, and J-Y. Lallemand, *J. Magn. Reson. B* **109,** 218 (1995).
16. D. Abergel, A. Louis-Joseph, and J.-Y. Lallemand, *J. Biomol. NMR* **8,** 15 (1996).
17. P. Broekaert and J. Jeener, *J. Magn. Reson. A* **113,** 60 (1995).
18. D. Abergel, A. Louis-Joseph, and J.-Y. Lallemand, *Chem. Phys. Lett.* **262,** 465 (1996).
19. V. Sklenar, *J. Magn. Reson. A* **114,** 132 (1995).
20. M. Piotto, V. Saudek, and V. Sklenar, *J. Biomol. NMR* **2,** 661 (1992).
21. V. Sklenar, M. Piotto,R. Leppik, and V. Saudek, *J. Magn. Reson. A* **102,** 241 (1993).
22. H. T. Edzes, *J. Magn. Reson.* **86,** 293 (1990).
23. A. G. Sobol, G. Wider, H. Iwai, and K. Wüthrich, *J. Magn. Reson.* **130,** 262 (1998).
24. A. J. Wand and D. L. Di Stefano, *Biochemistry* **28,** 186 (1989).
25. P. X. Qi, J. L. Urbauer, E. J. Fuentes, M. F. Leopold, and A. J. Wand, *Nat. Struct. Biol.* **1,** 378 (1994).
26. G. V. Louie and G. D. Brayer, *J. Mol. Biol.* **214,** 527 (1990).
27. A. M. Berghuis and G. D. Brayer, *J. Mol. Biol.* **223,** 959 (1992).
28. D. Marion, M. Ikura, R. Tschudin, and A. Bax, *J. Magn. Reson.* **85,** 393 (1989).
29. A. J. Shaka, C. J. Lee, and A. Pines, *J. Magn. Reson.* **77,** 274 (1988).